ISSN: 2634 - 8845

Journal of Earth and Environmental Science Research

SCIENTIFIC Research and Community

Research Article

Open Access

Mapping Analysis on Normalized Difference Vegetation Index (NDVI) Coverage and its Correlation with Land Surface Temperature Changes Utilizing Remotely Sensing Data and GIS in Southern Tigray Region, Northern Ethiopia

Fikre Hagos

Department of Geo-Informtics, Instiute of Geoinformation and Earth Observation Science, Mekelle University, Tigray, Ethiopia

ABSTRACT

The present study was conducted from 2015 to 2023, the objectives to analyze and detect changes in vegetation, to calculated NDVI, NDMI and LST values and correlation the NDVI and LST R2 produced for 2015 and 2023. were extracted from remotely sensed data (Landsat 8 Operational Land Imager (OLI)). The NDVI class covers the largest area at 1295.69 (40.77%), about the whole shown low vegetated area, and 1230.71 (38.86%) in 2015 and 2023, respectively. The values of -1.91 and -5.14 were decreased values. The 624.33 (19.64%) and 762.15 (24.06%) 2015 and 2023, respectively, moderate vegetation areas. The average NDVI value was a coverage of 4.42%, increasing in 2023 compared to 2015. The last NDVI class 245.26 (7.72%%) and 327.51 (10.34%) area was high vegetated the mean value 2.26 % coverage was changed or increasing in 2023 than 2015. LST was estimated using the conversion of radiance to satellite brightness temperature and spectral emissivity minimum, maximum, and mean values of LST. As we observe the mean results increasing from 25.470°C to 27.890°C in 2023 compared to 2015. The soil moisture coverage has been changed and decreased from 417.91 km^2 to 413.92 (-0.13%), and the low NDMI values also decreased from 1168.94 to 1166.24 (-0.09%); the very low and moderate NDMI values were increasing from 701.67 to 707.59 (0.19%) and 889.89 to 890.46 (0.05%), respectively, in 2015 and 2023. the study area was coverage 36.78 % and Moderated area was coved 27.899% moisture content covergs have less in area coveregs b/n 2015 and 2023. R^2 values for NDVI and LST correlations indicated 0.9634 in 2015 and 0.9587 in 2023, respectively, due to the differences in NDVI values.

***Corresponding author**

Susan Unyi Eru, Department of Environmental Sustainability, Joseph Sarwuan Tarka University Makurdi Benue State, Nigeria.

Received: February 24, 2025; **Accepted:** February 28, 2025; **Published:** March 10, 2025

Keywords: Surface Tempraure, NDVI, Landsat 8 OLI

Introduction

The Surface Temperature is directl connection with the earth temperature using determining instrument usually measured in °C. Surface Temperature was the earth's crust where the heat and radiation from the sun absorbvation and reflectance. It was a change in climatic condition and other human activities where the exact expectation becomes challenging [1]. Earth Temperature is one of the main variables, refer to surface processes and states severe in investigations of hydrology, weather, environmental science and human health [2]. In remote sensing, there are many satellites equipped with sensors operating within the infrared heat range [3]. Identification and characterization of the Heat Island (UHI) is typically based on Surface Temprature that varies spatially, due to the non-homogeneity of land surface cover and other atmospheric factors. The surface temperature has increased due to the conversion of Land Use Change to no evaporating surfaces [4]. There are many studies in this area in different country by different method. However, few studies have been carried out to estimate of climatic parameters for urban climatology (LST) inEthiopia. According to Bedada, this research article investigate the relation between LST and NDVI by using Landsat in Addis Ababa city [5]. Because various Land surfaces Temperature emit and absorb energy radiation in different ways, they have been studied in order to determine LST [6]. Land surface Temperature (LST) and emissivity for large area can only be derived from surface-leaving radiation measured by satellite sensors [7]. LST is the key factor for calculating highest and lowest Temperature of a particular location. LANDSAT 8 carries two sensors, i.e., the Operational Land Imager (OLI) and the Thermal Infrared Sensor (TIRS). OLI collects data at a 30m spatial resolution with eight bands located in the visible and near-infrared and the shortwave infrared regions of the electromagnetic spectrum, and an additional panchromatic band of 15m spatial resolution. TIRS senses the TIR radiance at a spatial resolution of 100m using two bands located in the atmospheric window between 10 and 12 µm [8]. In this study, NDVI and LST were found to be closely correlated in NDVI categories, especially in vegetated areas. Decrease of biomass primarily triggered on LST [9].

Recently, some investigations found the relationship between NDVI and vegetation abundance to be nonlinear. And this nonlinearity recommend NDVI may not be a competent indicator for quantitative analyses of vegetation [10]. So, the relationship between the LST and NDVI should be further calibrated. And seeking a more suitable and robust vegetation abundance indicator to supersede NDVI in Vegetation–LST relationship study should

be placed more emphasis [11]. In the study used satellite data investigate the relationship between Land Surface Temperature (LST) and vegetation in the Area. In our area no research conducted specifically focused on Geo-Spatial analysis for estimation of Land surface Temperature using remote sensing data. Numerous environmental conditions, including soil saturation, cloud cover, air particles, and the structural characteristics of a particular sensor, have been demonstrated to have an impact on the NDVI value [12]. The water stress level in plants is characterized by the NDMI [13]. Most frequently, this measure is employed to track vegetation moisture content and drought stress [14]. NDMI and its variations have proven effective in various vegetation study and classification contexts [15,16]. Therefore, This study's main goal is to apply the Mapping of Normalized Difference Vegetation Index (NDVI), Normalized Difference Vegetation Index (NDMI) indices to track change in vegetation condition and To retrieve Land Surface Temperature (LST) values and correlation NDVI and LST map between 2015 and 2023.

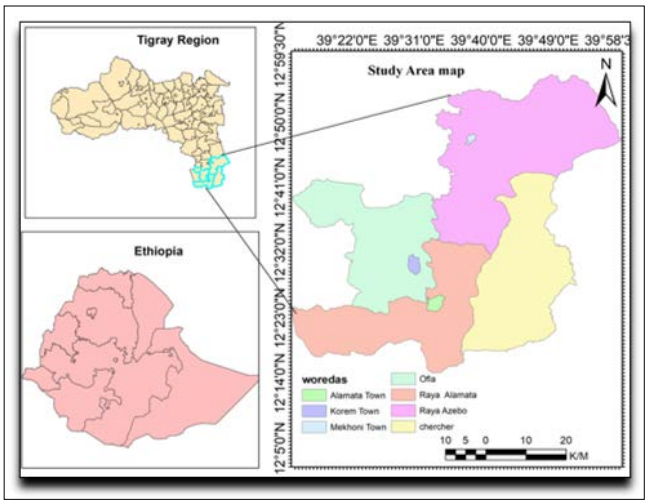

Figure 1: Location of the Study Area

Materials and Methods

Description of Study Area

Location

The present study, conducted from 2015 to 2023, aims to analyze and detect changes in vegetation using the Normalized Difference Vegetation Index (NDVI), Normalized Difference Moisture Index (NDMI) and Land Surface Temperature (LST) is processed from Landsat 8 imagery in Southern Tigray. The study area Located between between 120 0' 0" to 120 59' 30" North and 390 22' 0" to 400 1' 0" East longitude, in northen Ethiopia. The total area coverage are 317,834.17ha.

Design the Study

Land Surface Temperature (LST) assessment was produced from the Thermal bands, and lastly the results are combined to relationship LST and NDVI values. The flow chart represents the method that was used in this study (Figure 2). It demonstrates the processes taken to extract the required information, beginning with the acquisition and classification of a multi-temporal satellite image. Finally, Relationship analysis NDVI and ST was performed.

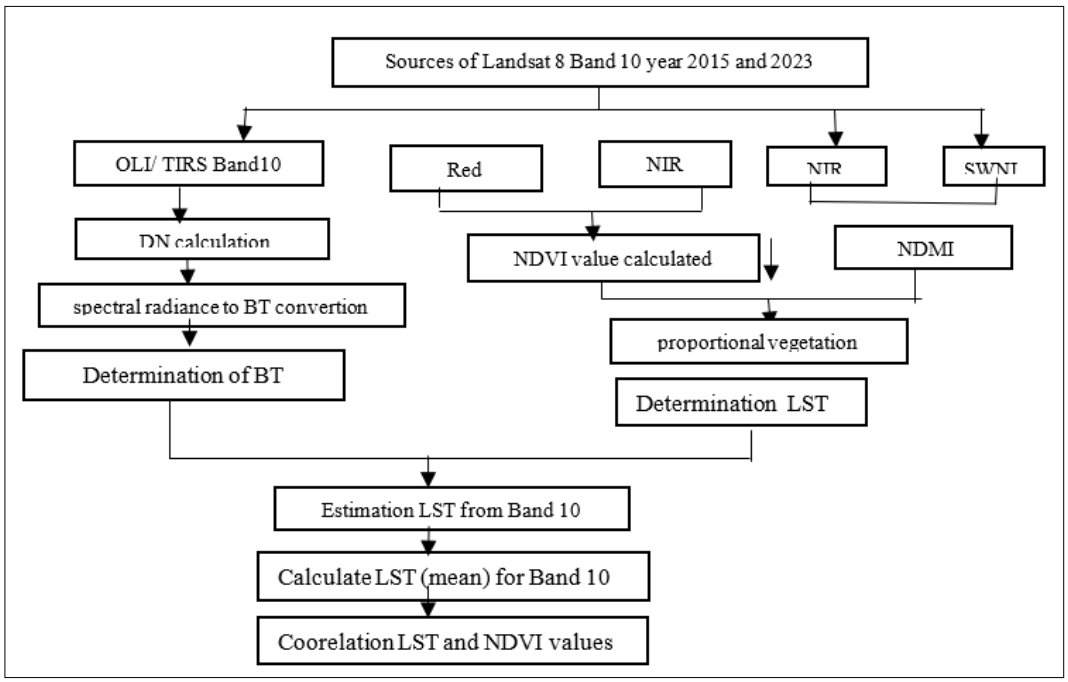

Figure 2: Methodological Flow Chart

Data Collection and Analysis

Methods of Data Collection

The remote sensing data was available in USGS (United States Geological Survey) Earth Explorer website at free of cost. When we were using those path and row 169/051during the month January for 2015 and 2023 years relatiliy free haz and cloud downloaded. The TIR bands 10 were used to estimate brightness temperature and bands 4 and 5 were used to generate NDVI of the study area. Landsat 8 provides metadata of each bands such as thermal constant, rescaling factor value etc. which can be used for Calculation Brightness Temperature, NDVI values and LST.

Table 1: LANDSAT 8_OLI & TIRS Meta Data

Bands	Wavelength (micrometers)	Resolution in meter
Band 4 Red	0.636 – 0.673	30
Band 5 NIR	0.851 – 0.879	30
Band 6 SWIR	1.57 – 1.65	30
Band 10 TIR-1	10.60 – 11.19	100

Following Meta data values are used for calculation
Radiance Add Band 10 = 0.10000
Radiance Mult Band_10 = 0.0003342
K1 Constant band 10 = 774.8853
K2 Constant Band 10 = 1321.0789

Method of Data Analysis

There are several steps or analytical procedures to be followed in order to conduct LST estimation and analysis. Conversion of DN values into Top of Atmosphere Radiance is the first step in land surface temperature estimation.in this algorism all, the satellite data were geometrically corrected and band 10 was used as an input data. In this activity radiance, rescaling factor is very important to retrieve the top of atmospheric (TOA) spectral radiance from Thermal Infra-Red Digital Numbers.

In order to estimate the land surface temperature from the thermal infrared band, DN of sensors are converted to spectral radiance using the following equation [17].

$$L\lambda = ML * Qcal + AL - OI$$

Where,

- ML represents the band specific multiplicative recalling factor
- Qcal is the Band 10
- AL is the band specific additive rescaling factor
- OI is the correction value for band 10 [18]

Conversion of Radiance to Brightness Temperature

After spectral radiance was converted to radiance, the raw DN of the thermal bands are converted to Brightness temperatures (BT) using the thermal constants given in the metadata, which is the effective temperature viewed by the satellite under an assumption of uniform emissivity [19]. If the resulte is in kalvin we should be to convert to in Celsius, it is necessary to revise by adding absolute zero which is approximately equal to -273.15. Since the atmosphere in our research is comparitively dry and therefore, the range of water vapor values is relatively small, the atmospheric effect is not taken into consideration in retrieving the LST. The equation used to convert reflectance to Brightness Temperature (USGS 2013).

$$BT = \frac{K2}{\ln\left[\left(\frac{K1}{L\lambda}\right)+1\right]} - 273.15$$

Where:

- BT = Top of atmosphere Brightness Temperature (°C)
- Lλ = TOA spectral radiance (Watts/(m^2 * sr * μm))
- K1= Band specific thermal conversion constant (K1_ constant_Band 10, thermal band)
- K2= Band specific thermal conversion constant from the metadata (K2_ constant_Band 11, thermal band)
- ln = natural logarithm

Normalized Difference Vegetation Index

we were used to calculate the NDVI valuve for the study area for 2015 and 2023. The normalized difference vegetation index is also used to predict general vegetation conditions and calculate the LST. The red band (high absorption of radiation or low reflection) and the infrared band (low absorption of radiation or high reflection) were used to calculate the NDVI. Green leaves have a reflectance of 20% or less in the 0.5 to 0.7-micrometer range and about 60% in the 0.7 to 1.3 range [20]. Therefore, NDVI values represent ratios ranging from -1.0 to 1.0.

$$NDVI = \frac{(NIR - RED}{(NIR + RED)}$$

Where:

- RED = DN values from the Red band (Band 4)
- NIR= DN values from Near-Infrared band (Band 5)

The next step is calculating proportional vegetation (Pv), this was done using the normalize difference vegetation index values or result obtained in the above step. This proportional vegetation helps to estimate the area under each land cover type in the study area [21]. Thus, proportional vegetation (Pv) can be calculated using the following equation. The experiment continued to locate the vegetation by setting the threshold of NDVI image.

$$Pv = \left(\frac{nNDVI - NDVIs}{NDVIv - NDVIs}\right)2$$

Where:

- PV = Proportion of Vegetation
- NDVI = DN values from the Image.
- NDVI min = Minimum DN values from the Image.
- NDNI max = Maximum DN values from the Image.

Land Surface Emissivity

The land surface emissivity (LSE (ε)) must be known because LSE is a proportional factor that scales blackbody radiance to predict emitted radiance. In satellite images, pixels representing the land surface are usually mixed pixels, they are a combination of surfaces-types such as water, vegetation, and soil. Therefore, the effective emissivity of a pixel can be calculated by summing up the contributions from those surface types because the emissivity value change from surface to surface. Land surface emissivity is the Earth's average surface factor emissivity determined from the standardization of vegetation index values for variations. Corrections for emissivity (e) have applied to the radiant temperatures according to the nature of land cover [21]. Though to estimate the emissivity from satellite thermal band quite a lot of methods have been suggested, the NDVI threshold method was used in this study. Land surface emissivity was calculated via the following formula.

$$\varepsilon = \varepsilon v\lambda Pv + (1 - Pv) + C\lambda$$

Where:

- E = Land Surface Emissivity
- EVλ = emissivity of vegetation
- ES λ= emissivity of soil
- PV = proportion of vegetation
- Cλ = surface roughness taken as a constant value of 0.005

Where εv and εs are the vegetation and soil emissivity respectively, C is the surface roughness taken as a constant value of 0.005 [22]. Studies conducted by Jose A. show that the emissivity of water bodies is utmost stable in comparison with land surfaces. Since the emissivity depends on the wavelength, the Normalize Difference Vegetation Index can be used to estimate the emissivity of different land surfaces in the 10-12 μm range. Then, we calculating Land Surface Temperature (LST) is the final steps in this algorism. The surface temperature value of the study area can be calculated as this equation.

$$LST = TB/(1+(\lambda * TB/c) * \ln(e))$$

Where

BT = Brightness value of atmospheric temperature (°C), W = Wavelength of emitted radiance in meters (for which the peak response and the average of the limiting wavelengths (λ = 11.5lm) [23].

The Normalized Difference Moisture Index (NDMI)

The NDMI value can be estimated from Landsat 8 imagery which can then be analysed from Band 5 with a Near-Infrared sensor and Band 6 with a ShortWave sensor. The ratio between the difference and the sum of the reflected radiations in the SWIR and NIR were used to calculate the NDMI, which measures the plant's water stress. Using equation 2, the NDMI was generated with band 5 as the NIR and band 6 as the SWIR [13].

$$NDMI = \frac{NIR - SWIR}{NIR + SWIR}$$

Validation of Retrieved Land Surface Temperature

As the Earth's surface temperature is determined from thermal remote sensing datasets utilizing dynamic methods and underlying hypotheses regarding atmospheric parameters, it is also important to determine its precision, which is beneficial for both consumers and engineers. According to, Normal land surface temperature products of the same region and same time in ethiopia can be used to confirm the obtained surface temperature values [24]. Yet due to the complex existence of land surface temperature, both spatially and temporarily, ground-based values cannot be obtained to crossvalidate the temperature of the collected surface. Furthermore, owing to the non-availability of observed surface temperature details, the cross-validation technique was used to confirm the recovered surface temperature of the earth; thus we used regular data sets of Landsat 8- OLI earth surface temperature products with precision within 1oK range to confirm the earth surface temperature of Landsat 8 satellite image [25].

Land Surface Temperature (LST) is processed from Landsat 8 imagery using bands 10 because these bands can convert the digital number obtained from the image metadata to radians and then convert it in kelvin units. Kelvin temperature values will later be converted back to centigrade units this process is done digitally.

Results and Discussion

The present study has been conducted on Agricultural area, Vegetative, Settlement and urban area. The level of vegetation coverage also have factor for the Temperature incrseanig. The value of NDVI is also divided in to vegetated area, semi vegetated and areas. Normally the value of NDVI range from positive 1 to negative -1. The middle values is approximately zero values represent non – vegetated lands while positive values represent vegetated area. The NDVI result to show the distribution of the vegetation in the study area coverage from 2015 to 2023 respectively. The Land Surface Temperature (LST) was radiates temperature which calculated using Top of atmosphere brightness temperature, Wavelength of emitted radiance, Land Surface Emissivity.

Normalize Difference Vegetation Index Map

The output value of NDVI values we area classify in to four ranged between -0.158 - 0.570, 0.065–0.512 for 2015 and 2023 respectivily show in (Figure 3). Higher value of NDVI shows the more dense vegetation (plantation), respectively. The NDVI is mainly an indicator that utilizes the Near-Infrared (NIR) bands in the electromagnetic spectrum to assess and analyze healthy vegetated areas. Generally, healthy vegetated areas absorb most of the sun's visible light and reflect a large portion of the NIR to space. On the other side, barren soils reflect moderately in both the NIR and the red portion of the electromagnetic spectrum [26]. So, Negative values usually represent water body, around zero represent barren soil, whereas values over 0.5 usually represent green vegetated areas. As indicated in (Figure 3) vegetation cover has decreased and the non-vegetated area has been increasing gradually over the study period 2023. However, in 2023 both in rural and urban areas have low NDVI values.

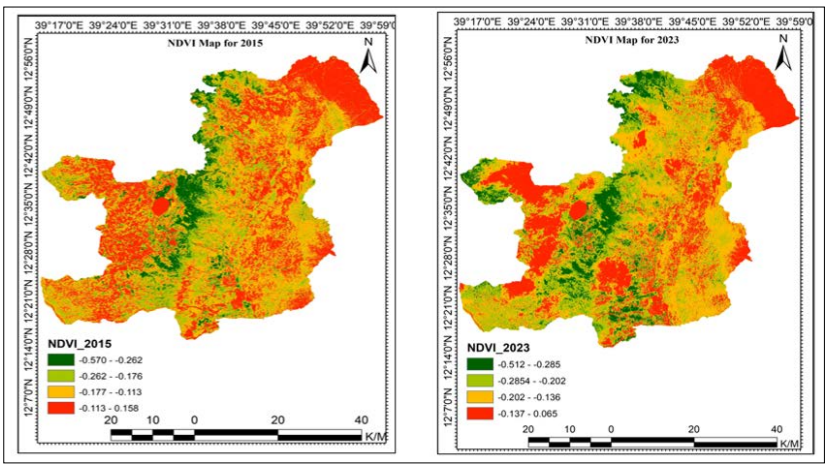

Figure 3: NDVI values for 2015 and 2023

The NDVI value covered classified classes to show (Table 2) the largest area coverge1295.69 (40.77%) about the hole shown low vegetated area and 1230.71 (38.86%) in 2015 and 2023 respectivily years show that low, therefore, the average value of -1.91 and -5.14 it shows decreased area classes. The 624.33 (19.64%) and 762.15 (24.06%) 2015 and 2023 respectivliy year moderate vegetation areas.the mean NDVI values was coverage 4.42% increasing in 2023 than 2015. The last NDVI class 245.26 (7.72%%) and 327.51 (10.34%) area was high vegetated the mean value 2.26 % coverage was changed or increasing in 2023 than 2015.

Table 2: Changes NDVI Vlues Area Coverges between 2015 and 2023

NDVI class	2015 Area (km^2)	coverage in %	2023 Area (km^2)	coverage in	Change 2015 -2023 in %
V.Low Veg.	1013.04	31.87	846.75	26.74	- 5.14
Low Veg.	1295.694	40.77	1230.71	38.86	- 1.91
Moderate Veg.	624.326	19.64	762.15	24.06	+4.42
High Veg.	245.262	7.72	327.51	10.34	+2.62
Total Area	3178.32	100	3178.32	100	3178.32

Land Surface Temperature (LST) Analysis

Land surface temperature (LST) acquired from Landsat-8 thermal band 10, has been done in ArcGIS Application and LST maps of the study area were produced show in (Figure 4). The different thermal signatures seen in the LST maps of the area because of the different land cover classes having different physical properties.

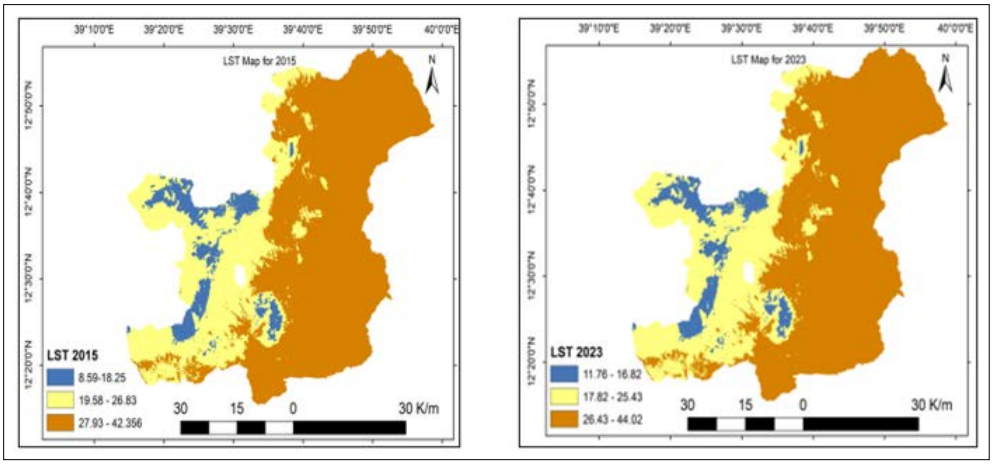

Figure 4: Classify Surface Temperature Map for 2015 and 2023

LST was estimated using conversion of radiance to At satellite brightness temperature and spectral emissivity. It shows in (Table 3) minimum, maximum and Mean values of Land Surface Tempture. As we observation the mean results increasing from 25.47^{0}C to 27.89^{0}C on 2023 than 2015. So, The temperature value for 8 years for the area was generally incrising in from min and max Tempratures.

Table 3: LST vlues in Min, Max and Mean for June 2015 And June 2023

	2015	2023
Temp	**Temp in^{0}C**	**Temp in^{0}C**
Max	42.356	44.02
Mean	25.47	27.89
Min	8.585	11.77

The Normalized Difference Moisture Index (NDMI)

The Normalized Difference Moisture Index (NDMI) surface moisture index is used to evaluate the different humidity of elements of a landscape. The NDMI value can be estimated from the previously downloaded Landsat 8 imagery which can then be analysed from Band 5 with a Near-Infrared sensor and Band 6 with a ShortWave sensor. The map of NDMI values can be obtained from the results processed using ArcGIS software with we are stated on the methodology formula.

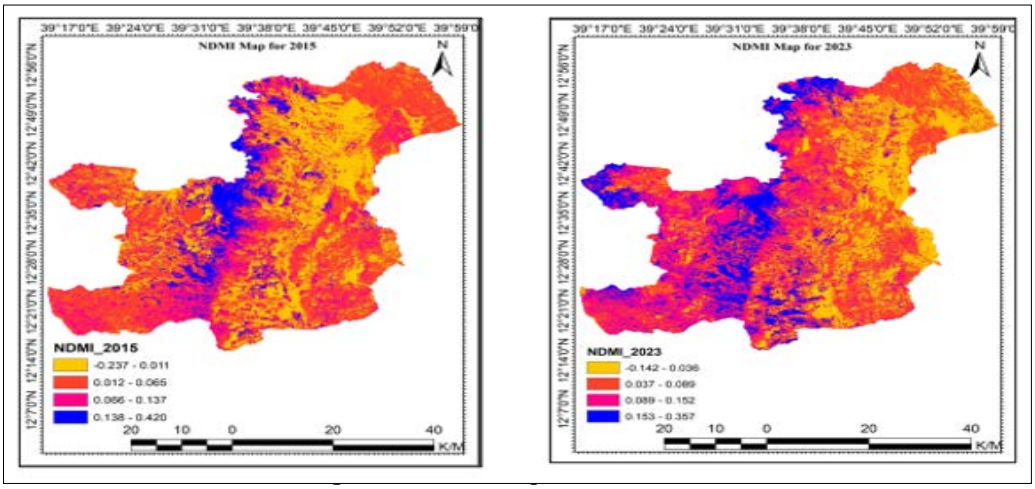

NDMI Values btween 2015 and 2023

The soil mosture covereged has been changed significantly between 2015 and 2023. Affording to the NDMI maps, the high amount of moisture content have slightly Dcreased from 417.91km^2 to 413.92 (-0.13%) and the low NDMI values also decresed from 1168.94 to 1166.24 (-0.09%), the very low and moderated NDMI values were increseing from 701.67 to 707.59 (0.19%) 889.89 to 890.46 (0.05%) respectively the year 2015 and 2023. the study area was coverage 36.78 % and Moderated area was coved 27.899% moisture content covergs have less in area coveregs show in (Tables 4).

Table 4: Changes NDMI Vlues Area Coverges between 2015 and 2023

NDMI Class	2015 Area (km^2)	Covarage in %	2023 Area (km^2)	Covarage in %	Change 2015 -2023 in %
V.Low NDMI.	701.67	22.08	707.59	22.26	0.19
Low NDMI.	1168.94	36.78	1166.24	36.69	-0.09
Moderate NDMI.	889.89	27.899	890.46	28.05	0.05
High NDMI	417.91	13.15	413.92	13.02	-0.13
Total Area	3178.32	100	3178.32	100	

Surface Temperature and NDVI Correlation

The LST and NDVI correlation generated from Landsat 8 themal bands 10 and for 2015 and 2023 have shown that NDVI values and LST values obtained from the Thermal bands for 2015 and 2023 had indicated an indirect relationships between them see (figure 6). However, the relationship between NDVI and LST showed direct/positive relationship for water body, because both NDVI and ST values were less for water body. The R^2 values for the NDVI and LST correlations indicated 0.9634 in 2015 and 0.9587 in 2023, respectively due to the differences in NDVI value for the years concerned. According to, NDVI is an acceptable indicator of Surface Temprature [27]. There are a number of factors contributing to an increase or decrease Surface Temprature value of the area.

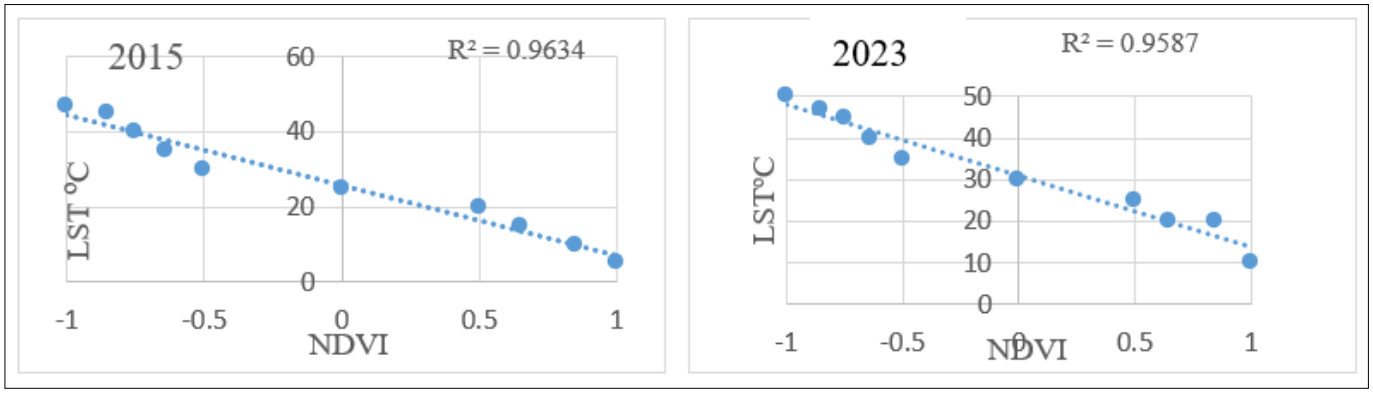

Figure 6: Correlation NDVI and LST for 2015 and 2023

Conclusion

Landsat 8 thermal bands 10 for 2015 and 2023, it has been shown that NDVI and LST values obtained from the thermal bands have indicated an indirect relationship between them. The NDVI class covers the largest area at 1295.69 (40.77%), about the whole shown low vegetated area, and 1230.71 (38.86%) in 2015 and 2023, respectively. The values of -1.91 and -5.14 were decreased values. The 624.33 (19.64%) and 762.15 (24.06%) 2015 and 2023, respectively, moderate vegetation areas. The average NDVI value was a coverage of 4.42%, increasing in 2023 compared to 2015. The last NDVI class 245.26 (7.72%%) and 327.51 (10.34%) area was high vegetated the mean value 2.26 % coverage was changed or increasing in 2023 than 2015.LST was estimated using the conversion of radiance to satellite brightness temperature and spectral emissivity minimum, maximum, and mean values of LST. As we observe the mean results increasing from 25.470°C to 27.890°C in 2023 compared to 2015. The soil moisture coverage has been changed and decreased from 417.91 km² to 413.92 (-0.13%), and the low NDMI values also decreased from 1168.94 to 1166.24 (-0.09%); the very low and moderate NDMI values were increasing from 701.67 to 707.59 (0.19%) and 889.89 to 890.46 (0.05%), respectively, in 2015 and 2023. The study area was covered 36.78%, and the moderated area was covered 27.899%. Moisture content coverage has decreased in area coverage between 2015 and 2023. The R^2 values for the NDVI and LST correlations indicated 0.9634 in 2015 and 0.9587 in 2023, respectively, due to the differences in NDVI value for the years concerned [28-38].

Acknowledgement

The an authors would like to thank you Mekelle university instiuted of Geoinformation and Earth Observasion science (I-GEOS) for data and Technical support to compulet this arthicl work.

References

1. Bhatt JP (2012) Estimating Temporal Land Surface Temperature Using Remote Sensing A Study of Vadodara Urban Area, Gujarat. International Journal of Geology, Earth and Environmental Sciences. https://www.semanticscholar.org/paper/ESTIMATING-TEMPORAL-LAND-SURFACE-TEMPERATURE-USING-Joshi-Bhatt/7196be2f470bebff82298e8f03a2c5196159241c.
2. Du CR (2015) A practical split-window algorithm for estimating land surface temperature from Landsat 8 data. Remote Sensing 7: 647-665.
3. Ghazal NK (2012) Temperature Calculation Using Thermal Bands Of (ETM+) Sensor. Iraqi Journal of Science 53: 435-443.
4. Sahana MA (2016) Analyzing land surface temperature distribution in response to land use/land cover change using split-window algorithm and spectral radiance model in Sundarban Biosphere Reserve, India. Modeling Earth Systems and Environment 2: 81.
5. Bedada B (2017) Estimation of Land surface Temperature Using Landsat by split window Algorithm: A Case study in Bahir Dar Zurya, Ethiopia. Journal of Envornment and Eath Science 7: 5.
6. Pongratz JR (2010) Biogeophysical versus biogeochemical climate response to historical anthropogenic land cover change Geophys. Res Lett 37: 02-09.
7. Prasanjit DF (2002) Land surface temperature and Emissivity Estimation from Passive sensor Data: Theroy and Practice–Current Trends. International Journal of Remote sensing 23: 2563.
8. Anandababu D, Purushothaman BM, Suresh Babu S (2018) Estimation of Land surface Temperatue using LANDSAT 8 Data. Inernational journal of advance research, ideas and innovation in technology 4: 177-186.
9. Manat Srivanit (2012) Assessing the Impact of Urbanization on Urban Thermal Environment: A case study of Bangkok metropolitan. International Journal of Applied Science and Technology 2: 243-256.
10. Su wei YD (2013) Vegetation change in the agricultural pastoral areas of no china from 2001 to 2013. Journal of Integrative Agricultural 15: 1145-1156.
11. Amson (2018) Urban green areas to Mitigate Urban heat Island Effect: the case of Addis Ababa, Ethiopia. Int J Ecol Environ Sci 44: 353-367.
12. Anonymous (1999) MODIS Vegetation index (MOD 13) algorithm theoretical basis document. https://modis.gsfc.nasa.gov/data/atbd/ atbd_mod13.pdf.
13. Gao B (1996) NDWI-A normalized difference water index for remote sensing of vegetation liquid water from space. Remote Sensing of Environment 58: 257-266.
14. Nasiłowska SK (2016) Zmiennosc wskazników NDVI oraz NDMI na przykładzie analizy uprawy kukurydzy w Etiopii. Teledetekcja Srodowiska 55: 15-26.
15. Khanna SS (2013) Detection of salt marsh vegetation stress and recovery after the deepwater horizon oil spill in barataria bay, Gulf of Mexico Using. https://doi. org/10.1371/journal.pone.0078989.
16. Mabrur AS (2019) Remote sensing technology for land farm mapping based on NDMI, NDVI and LST feature. International Journal of Innovative Technology and Exploring Engineering 3: 75-79.
17. Suresh S, Suresh A, Mani K (2015) Analysis of land surface temperature variation using thermal remote sensing spectral data of Landsat satellite in Devikulam Taluk, Kerala-India. IJREAS 5: 145-154.
18. 18. Barsi (2014) The respecteral response of Landsat -8 Operational Land Imajer. Remote Sensing 10232-10251.
19. Mani ND (2014) Estimation of LST of Dindigul district using LANDSAT 8 data. IJRET 3: 122-126.
20. Nigus Tekleselassie Tsegaye, Girma Alemu Melka (2022) Land surface Temperature detection in Relational to Land use land cover change in the case of jimma city ethiopi. https://www.researchsquare.com/article/rs-1388653/v1.
21. Jeevalakshmi (2017) Land surface temperature retrival from LANDSAT data using emissivity estimation. Journal of Applied Engineering Research 12: 9679-9687.
22. Peter Horvath, Rune Halvorsen, Frode Stordal, Lena Merete Tallaksen, Hui Tang, et al. (2019) Distribution modelling of vegetation types based on area frame survey data. Applied Vegatation Science 22: 547-560.
23. Jeevalakshmi D, Narayana Reddy S, Manikiam B (2016) Land cover classification based on NDVI using LANDSAT8 time series: A case study Tirupati region. IEEE International Conference on Communication and Signal Processing (ICCSP) 1332-1335.
24. Zhao (2013) Satellite derived land surface teperature; current stutus and perspectives. Remote Sensing Environment 14-37.
25. Qihao Weng, Dengsheng Lu, Jacquelyn Schubring (2004) Estimation of land surface temperature-vegetation abundance relationship for urban heat island studies. Remote Sensing of Environment 89: 467-483.
26. Yosef (2011) NIR-red reflectance-based algorithms for chlorophylly-a estimation in mesotrophic inland and coastal water. Water esearch 2428-2436.

27. Herbei M (2012) Using Satellite images landsat TM for calculating Normalized Difference Indexes for the landscape of Parang mountains. https://www.semanticscholar.org/paper/USING-SATELLITE-IMAGES-LANDSAT-TM-FOR-CALCULATING-Herbei/d80c9da52e3b8918b7af2f749ba51981a21dbf9e.
28. Achmad E (2018) Indeks kelembaban taman nasional bukit tiga puluh menggunakan citra satelit Landsat 8. Prosiding Seminar Nasional Geomatika 2018: Penggunaan dan Pengembangan Produk Informasi Geospasial Mendukung Daya Saing Nasional. Bogor 5: 425-432.
29. Charlie J Tomlinson, Lee Chapman, John E Thornes, Christopher Baker (2011) Remote Sensing Land Surface Temperature for Meteorology and Climatology: A Review. Meteorological Applications 18: 296-306.
30. Dede M (2019) Dinamika Suhu Permukaan Dan Kerapatan Vegetasi Di Kota Cirebon. Journal of Meteorology, Climatology and Geophysics 6 No 1 .
31. Narayana Reddy S, Jeevalakshmi Digavinti, Balakrishnan Manikiam (2017) Land Surface Temperature Retrieval from LANDSAT data using Emissivity Estimation. International Journal of Applied Engineering Research 12: 9670-9687.
32. Gebrekidan W (2016) Modeling land surface temperature from satellite data, the case of Addis Ababa. the case of Addis Ababa. In: ES RI, Eastern Africa Education GIS conference 23-24.
33. Jose A Sobrino, Juan C Jimenez Munoz, Guillem Soria, Mireia Romaguera, Luis Guanter, et al. (2008) Land Surface Emissivity Retrieval from Different VNIR and TIR Sensors. IEEE Transactions on Geoscience and Remote Sensing 46: 316-327.
34. Liu L, Yuanzhi Zhang (2011) Urban heat island analysis using the Landsat TM data and ASTER data: A case study in Hong Kong. Remote Sens 3: 1535-1552.
35. Roberts DA, Philip E Dennison, Keely L Roth, Kenneth Dudley, Glynn Hulley (2015) Relationships between dominant plant species, fractional cover and land surface temperature in a Mediterranean ecosystem. Remote Sensing Environ 167: 152-167.
36. Stathopolou (2007) Daynamic urban heat Islands from Landsat ETM and corine Land cover data. An application to major cties in greence solar energy 358-368.
37. Vermote EF (1997) Second Simulation of the Satellite Signal in the Solar Spectrum, 6S: An overview. IEEE Transactions on Geoscience and Remote Sensing 35: 675-686.
38. Wan Z (1996) Generalized split-window algorithm for retrieving land surface temperature from space. Transactions on Geoscience and Remote Sensing 34: 892-905.